ChemComm

COMMUNICATION

View Article Online
View Journal | View Issue

Cite this: *Chem. Commun.*, 2025, **61**, 13908

Received 13th June 2025,
Accepted 5th August 2025

DOI: 10.1039/d5cc03353e

rsc.li/chemcomm

PFOA induces fission of phase-separated phospholipid vesicles

Seungsu Han,† Emad Pirhadi,† Xin Yong * and Sangwoo Shin *

Per- and polyfluoroalkyl substances (PFAS) are known for their strong surface activity, making it easy for them to disrupt cellular membranes. Here, we examine how perfluorooctanoic acid (PFOA), one of the most widespread PFAS species in the environment, interacts with phase-separated ternary vesicles as a model system for cellular membranes. We show experimentally that PFOA induces rapid fission of the vesicles along the phase boundary. All-atom molecular dynamics simulations suggest that the mechanism behind the fission process is attributed to a drastic change in the spontaneous curvature of the vesicle upon interacting with PFOA. Our findings reveal the significance of PFAS on the dynamics of phase-separated vesicles, implying a potential disruptive impact of PFAS exposure on cellular membranes.

PFAS, often referred to as 'forever chemicals', are a class of emerging pollutants characterized by their persistence in the environment and their adverse effects on mammalian health. They are documented as a risk factor for cancer.[1,2] Over the past decade, growing concerns about the widespread presence of PFAS in the biosphere have led to extensive investigations on the biological impact of PFAS.[3–5] In particular, a series of studies identified that PFAS can penetrate and alter the properties of phospholipid bilayers and cellular membranes.[6–11] This behavior has been attributed to the strong hydrophobicity of the fluorinated tail group of PFAS.

In cellular membranes, phase separation occurs spontaneously due to the energetic preference between different lipid species.[12] In this study, we hypothesize that PFAS can interfere with phase-separated domains in membrane vesicles, as their strong amphiphilicity may change the composition and physical properties of plasma membranes.[8] Induced membrane perturbations can potentially lead to suppression of normal cellular operations since many key cellular functions, including cell signaling, nutrient exchange, and trafficking, rely on the existence of phase-separated domains of plasma membranes.[13–15]

Previous studies have focused on the interaction of PFAS with single-phase vesicles or supported bilayers. There is a critical knowledge gap regarding the impact of PFAS on the dynamics of membrane phase separation, as the interaction between PFAS and multiphase vesicles remains poorly understood. Here, combining experiments involving ternary (DOPC/DPPC/Chol = 2 : 2 : 1) vesicles and perfluorooctanoic acid (PFOA), all-atom molecular dynamics (MD) simulations of equivalent bilayer systems, and a free energy analysis, we show that PFOA disrupts the dynamics of phase-separated vesicles and induces a morphological transition.

Upon introducing PFOA (concentration = 1 mM) to phase-separated giant unilamellar vesicles (GUVs) (see SI for details), we observed rapid fission of GUVs (Fig. 1(a) and Movie S1, SI). Initially at equilibrium, GUVs exhibit a Janus-like spherical morphology with each hemisphere constituting liquid-ordered phase (L_O; dark) and liquid-disordered phase (L_D; bright). The angle formed between the two phases (θ) is approximately 90° (Fig. 1(b)). Once GUVs are exposed to PFOA, θ gradually increases until the vesicle hemispheres divide into two distinct vesicles; one in the liquid-ordered and the other in the liquid-disordered phase. This process lasts for approximately 150 seconds. For comparison, the same concentration of octanoic acid solution was introduced to the phase-separated GUVs (Movie S2, SI). Despite sharing an identical head group and molecular structure to PFOA, except for its hydrocarbon tail, octanoic acid did not induce any visible morphological change in the GUVs. This control experiment eliminates the possibility of other minor effects such as osmotic pressure,[16,17] electrostatic charge,[18] or tail length.[19]

Interestingly, there exist equilibrium states of θ sensitive to PFOA concentration, implying that PFOA-induced fission is not triggered by mechanical instability, but rather determined thermodynamically (Fig. 1(b)). With higher PFOA concentrations, θ increases until it reaches the critical concentration where fission occurs (1 mM), *i.e.*, a larger amount of PFOA

Department of Mechanical and Aerospace Engineering, University at Buffalo, The State University of New York, Buffalo, New York, 14260, USA.
E-mail: xinyong@buffalo.edu, sangwoos@buffalo.edu
† These authors contributed to this work equally.

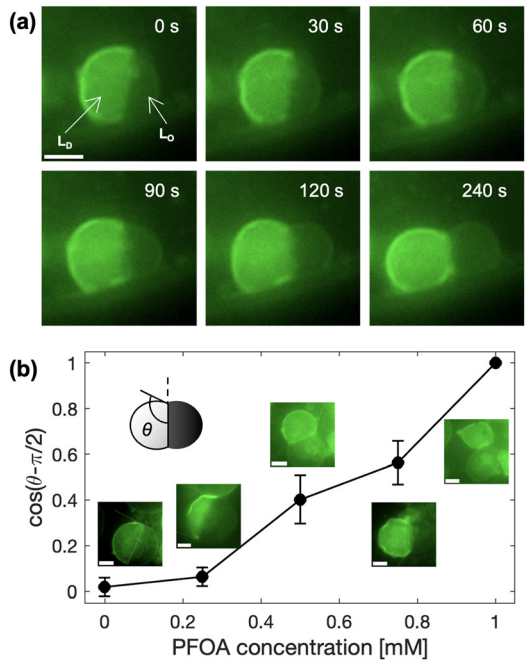

Fig. 1 PFOA induces fission of phase-separated GUVs (DOPC/DPPC/Chol = 2 : 2 : 1). (a) A sequence of fluorescence images of fission of phase-separated GUV upon introduction of 1 mM PFOA (Movie S1, SI). (b) Equilibrium θ as a function of surrounding PFOA concentration. Scale bars are (a) 10 μm and (b) 20 μm.

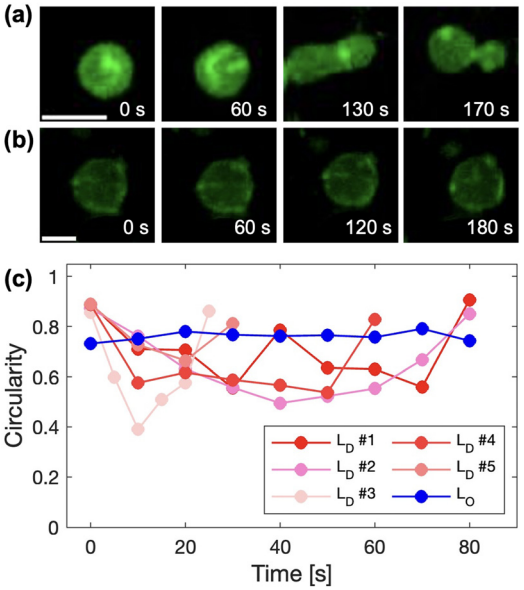

Fig. 2 Impact of PFOA on DOPC/Chol and DPPC/Chol vesicles. (a) and (b) Budding and division of (a) DOPC/Chol (Movie S3, SI) and (b) DPPC/Chol GUVs (Movie S4, SI) after PFOA introduction. (c) Circularity change of DOPC/Chol (L_D) and DPPC/Chol (L_O) binary vesicles. Scale bars are 10 μm.

molecules surrounding the GUVs lead to a higher degree of vesicle fission.

Moreover, when the initially dilute PFOA solution is replaced by more concentrated PFOA solution, θ increases from its initial value and transitions to the new equilibrium θ (Movie S5, SI). This behavior suggests equilibrium partitioning of PFAS into the phospholipid bilayer,[20,21] which influences its phase behavior and vesicle fission process.

Notably, the ways in which PFOA interacts with each phase of the vesicle is different. We conducted separation experiments with binary GUVs corresponding to each phase in the ternary vesicle. PFOA induces a rapid morphological transformation in the DOPC/Chol (= 2 : 1) binary GUVs, leading to budding and subsequent division of the vesicle (Fig. 2(a) and Movie S3, SI).

To quantify the morphological transformation of the binary GUVs, evolution of vesicle circularity prior to completing the division is measured (Fig. 2(c)). The circularity Γ is defined as $\Gamma = 4\pi A/P^2$, where A and P are the cross-sectional area and the perimeter of a vesicle, respectively. The typical circularity of DOPC/Chol GUVs before PFOA exposure is measured to be close to unity, representing a spherical shape. As PFOA is introduced, the circularity decreases below 0.6 and then recovers its original value as the GUV is fully divided. This outcome suggests that the spontaneous curvature of DOPC/Chol GUVs has been altered due to PFOA penetration into the outer leaflet, where the spontaneous curvature is expected to increase with the amount of PFOA molecules inserted asymmetrically into the bilayer.[16,20]

On the other hand, DPPC/Chol (= 2 : 1) GUVs exhibit negligible morphological change compared to DOPC/Chol vesicles, indicating their stability against PFOA partitioning (Fig. 2(b) and Movie S4, SI). In fact, bilayers composed of DPPC and cholesterol are known to be more resistant to surfactant insertion.[22]

To provide a mechanistic understanding of PFOA-lipid interactions and the consequent change in the membrane properties, we perform all-atom MD simulations. We model two symmetric lipid bilayers composed of either DOPC/Chol or DPPC/Chol mixtures with a 2 : 1 lipid-to-cholesterol ratio, consistent with the experimental conditions (see SI for details). We characterize the free energy landscape of inserting a PFOA molecule into these membranes to assess its preferential interaction with different lipids.

The transmembrane potential of mean force (PMF) profiles of PFOA in DOPC/Chol and DPPC/Chol membranes are presented in Fig. 3. PMF quantifies the change in the system's free energy when PFOA is introduced to a certain normal position within the membrane with respect to when the molecule is in water.[23,24] The negative PMF well below the water/membrane interface indicates preferential interactions between PFOA and DOPC/Chol membrane, suggesting that PFOA would spontaneously insert into this membrane. In contrast, the free energy increases when PFOA penetrates the DPPC/Chol membrane, representing unfavorable interactions of PFOA with DPPC/Chol.

The distinct behavior of PFOA with the two membranes is attributed to the difference in lipid ordering. The double *cis* bonds introduce bends in the DOPC acyl chains, which prevent the tails from packing tightly and create gaps between neighboring lipids.[25] Compared with DPPC with straight hydrocarbon tails, DOPC provides the membrane with more accessible space to host PFOA. Accordingly, we argue that PFOA molecules

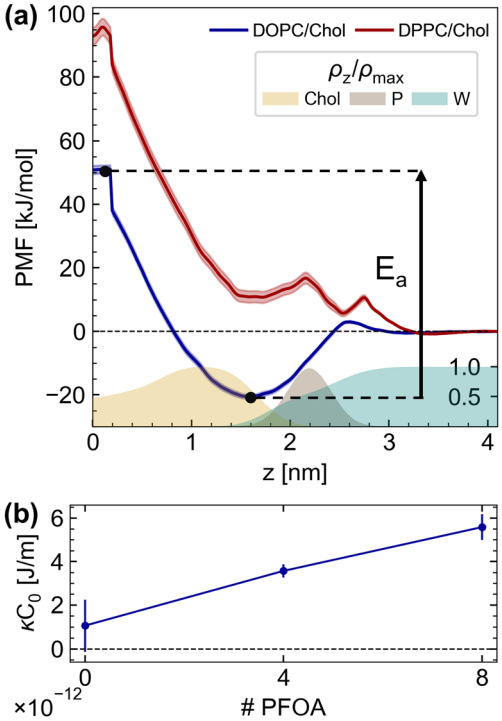

Fig. 3 PFOA preferentially partitions in the DOPC/Chol membrane and changes its curvature. (a) Transmembrane potential of mean force (PMF) profiles for PFOA interacting with the DOPC/Chol and DPPC/Chol membranes. The reaction coordinate (z) was defined as the distance between PFOA and the membrane's center of mass along the membrane normal direction. Scaled density profiles are depicted using shaded areas. E_a represents the activation energy for the flipping of PFOA from the outer to the inner leaflet of the DOPC/Chol membrane. The membrane center of mass is located at $z = 0$. The standard deviations of the PMF profiles are obtained from bootstrapping and represented with the shaded areas. (b) Torque density as a function of the number of PFOA molecules in the outer leaflet of the DOPC/Chol membrane. For a symmetric membrane, the torque density and thus the spontaneous curvature are zero.

will primarily insert into the DOPC-rich region of the ternary vesicle in our experiments. Hence, the subsequent fission behavior should be mainly due to the perturbation of the DOPC-rich domain.

To investigate whether PFOA induces mechanical deformation in the DOPC-rich domain of the ternary vesicle, we quantify the variations in the spontaneous curvature of the DOPC/Chol membrane with PFOA insertion. We model a set of DOPC/Chol membranes with varying PFOA concentrations in the outer leaflet of the membrane. These models mimic the experimental setup where PFOA is introduced to the vesicle from the exterior. We note that we do not expect PFOA flipping to the inner leaflet during the simulation time as the energy barrier (E_a) separating the two leaflets is $\sim$70 kJ mol^{-1} (Fig. 3(a)). For these systems, we calculate the torque density τ of the bilayer, which is equal to the first moment of the lateral stress profile (see eqn (S3), SI). The torque density is related to the spontaneous curvature through the equation $\tau = \kappa C_0$, with C_0 and κ representing the spontaneous curvature and the bending rigidity of the bilayer.

As shown in Fig. 3(b), with the addition of PFOA to the outer leaflet, the torque density of the membrane becomes positive. Since κ must be positive, the observed torque density corresponds to a positive spontaneous curvature. This result suggests that asymmetric insertion of PFOA into the outer leaflet could induce a positive spontaneous curvature in the DOPC-rich domain, facilitating its outward bulging and the fission of the ternary vesicle, as shown experimentally in Fig. 2(a).

Furthermore, the change in the total free energy of the phase-separated GUV verifies the hypothesis that vesicle fission is induced by the change in the spontaneous curvature.[17] The total free energy F_T of a phase-separated vesicle, which accounts for the Helfrich bending energy and the line tension, is given as

$$F_T = \sum_{i=1}^{n} \int 2\kappa^{(i)} \left(H^{(i)} - C_0^{(i)}\right)^2 dS + \int \gamma dl, \qquad (1)$$

where n, H, S, γ, and l are the number of phase domains, vesicle local mean curvature, phase domain surface, line tension, and phase boundary, respectively. Vesicle properties used for the calculations are summarized in Table S1, SI.

The initial state of the phase-separated vesicles with negligible spontaneous curvature ($\bar{C}_0 \approx 0$ m^{-1}; $\bar{C}_0$ is the area-averaged spontaneous curvature of the vesicle system) is marked at point 1 (Fig. 4). The free energy landscape indicates that this state with $\theta = 90^\circ$ is metastable. While the global minimum for zero-curvature vesicles is at $\theta = 180^\circ$ (*i.e.*, fission state), the free energy barrier due to the bending energy penalty prohibits vesicle fission. In fact, phase-separated GUVs remained stable experimentally for more than 12 hours at room temperature, further suggesting its metastability of the system.

However, assuming an increase in the spontaneous curvature of the vesicle upon exposure to PFOA solution, the contribution of bending energy diminishes effectively with curvature value above 2.5×10^4 m^{-1}, where the bending energy change would become negligible based on the calculated free energy landscape (Fig. S3). This results in the line tension emerging as the determinant factor for the morphology of phase-separated vesicles. In other words, the line tension facilitates the division of these domains because the energy

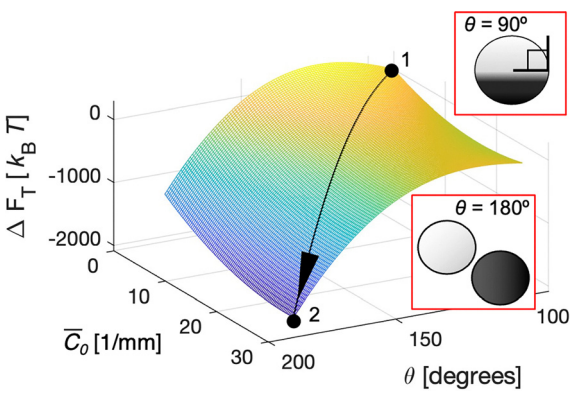

Fig. 4 Free energy landscape of the phase-separated GUV system. The GUV free energy landscape as a function of mean spontaneous curvature $\bar{C}_0$ and θ. Values are normalized to set initial state free energy zero.

barrier vanishes. As a result, the global minimum state of free energy can be reached. In essence, the asymmetric PFOA insertion triggers an energetically favorable fission of phase-separated vesicles.

To summarize, we have shown that phase-separated vesicles undergo an immediate fission when exposed to PFOA above a critical concentration, which is mainly due to the increase in the vesicle spontaneous curvature. In particular, PFOA partitioned preferentially into the outer leaflet of the DOPC/Chol membrane rather than the DPPC/Chol membrane, resulting in the curvature change. Notably, this phenomenon could be potentially critical for cellular functions, as the fission of phase-separated vesicles while conserving their surface area will in turn cause the loss of luminal contents from the daughter vesicles, such as organelles and enzymes. Such compromised integrity could adversely affect the membranes fundamental biological function as a selectively permeable barrier responsible for maintaining cellular homeostasis.[26,27] Furthermore, the shape alterations of vesicles might impair regulated vesicle trafficking pathways, disrupting essential cellular processes such as endocytosis, exocytosis, and intracellular transport.[28,29]

Albeit our free energy analysis has well validated that the fission state is a thermodynamically driven phenomenon, it inherently lacks full mechanistic understanding of the kinetics of the fission process, which should be addressed in the future. Also, while we utilized qualitative results from binary (single-phase) lipid vesicles to interpret the dynamics of ternary (phase-separated) lipid vesicles, the fact that phase-separated domains are still a mixture of ternary components[30] suggests a careful consideration of the results when analyzing the membrane dynamics quantitatively. We expect our work will potentially contribute to the understanding of the unresolved environmental and biological impacts of prevalent PFAS compounds.

This material is based upon work supported by the National Science Foundation under Grants No. 2237171 and 2448213. Computational resources of this research were provided by the Center for Computational Research at the University at Buffalo. Research reported in this publication was supported by SUNY System Administration under SUNY Research Seed Grant Award 241049.

Conflicts of interest

There are no conflicts to declare.

Data availability

The data supporting this article have been included as part of the SI.

Materials and methods, MD simulations, Table S1, Fig. S1–S3, Movies S1–S5. See DOI: https://doi.org/10.1039/d5cc03353e.

Notes and references

1 S. Kurwadkar, J. Dane, S. R. Kanel, M. N. Nadagouda, R. W. Cawdrey, B. Ambade, G. C. Struckhoff and R. Wilkin, *Sci. Total Environ.*, 2022, **809**, 151003.
2 G. M. Sinclair, S. M. Long and O. A. Jones, *Chemosphere*, 2020, **258**, 127340.
3 A. Wicks, H. D. Whitehead and G. F. Peaslee, *Environ. Sci. Technol. Lett.*, 2024, **12**, 25–30.
4 National Academies of Sciences, Engineering, and Medicine, *Guidance on PFAS Exposure, Testing, and Clinical Follow-Up*, 2022.
5 L. Ahrens and M. Bundschuh, *Environ. Toxicol. Chem.*, 2014, **33**, 1921–1929.
6 Z. Shen, J. Ge, H. Ye, S. Tang and Y. Li, *J. Phys. Chem. B*, 2020, **124**, 5415–5425.
7 M. Jbeily, R. Bärenwald, J. Kressler, K. Saalwächter and T. M. Ferreira, *Sci. Rep.*, 2018, **8**, 2154.
8 A. Naumann, J. Alesio, M. Poonia and G. D. Bothun, *J. Environ. Chem. Eng.*, 2022, **10**, 107351.
9 N. J. Fitzgerald, A. Wargenau, C. Sorenson, J. Pedersen, N. Tufenkji, P. J. Novak and M. F. Simcik, *Environ. Sci. Technol.*, 2018, **52**, 10433–10440.
10 E. D. Oldham, W. Xie, A. M. Farnoud, J. Fiegel and H.-J. Lehmler, *J. Phys. Chem. B*, 2012, **116**, 9999–10007.
11 S. Zheng, P. Sarker, D. Gursoy, T. Wei and B. S. Hsiao, *Langmuir*, 2025, **41**, 9369–9376.
12 R. Dimova, *Annu. Rev. Biophys.*, 2019, **48**, 93–119.
13 P. Sengupta, B. Baird and D. Holowka, *Semin. Cell Dev. Biol.*, 2007, 583–590.
14 T. Hamada, S. Mizuno and H. Kitahata, *Soft Matter*, 2022, **18**, 9069–9075.
15 S. L. Veatch and S. L. Keller, *Biochim. Biophys. Acta*, 2005, **1746**, 172–185.
16 Y. Miele, G. Holló, I. Lagzi and F. Rossi, *Life*, 2022, **12**, 841.
17 M. Andes-Koback and C. D. Keating, *J. Am. Chem. Soc.*, 2011, **133**, 9545–9555.
18 R. Bnyan, I. Khan, T. Ehtezazi, I. Saleem, S. Gordon, F. O'Neill and M. Roberts, *J. Pharm. Sci.*, 2018, **107**, 1237–1246.
19 N. Wongsirojkul, A. Masuta, N. Shimokawa and M. Takagi, *Membranes*, 2022, **12**, 781.
20 J. Steinkühler, R. L. Knorr, Z. Zhao, T. Bhatia, S. M. Bartelt, S. Wegner, R. Dimova and R. Lipowsky, *Nat. Commun.*, 2020, **11**, 905.
21 A. Mangiarotti, E. Sabri, K. V. Schmidt, C. Hoffmann, D. Milovanovic, R. Lipowsky and R. Dimova, *Nat. Commun.*, 2025, **16**, 1–20.
22 E. Schnitzer, M. Kozlov and D. Lichtenberg, *Chem. Phys. Lipids*, 2005, **135**, 69–82.
23 G. M. Torrie and J. P. Valleau, *J. Comput. Phys.*, 1977, **23**, 187–199.
24 E. Pirhadi, J. M. Vanegas, M. Farin, J. W. Schertzer and X. Yong, *J. Chem. Theory Comput.*, 2022, **19**, 363–372.
25 J. Pan, S. Tristram-Nagle and J. F. Nagle, *Phys. Rev. E*, 2009, **80**, 021931.
26 D. A. Ammendolia, W. M. Bement and J. H. Brumell, *BMC Biol.*, 2021, **19**, 71.
27 C. Dias and J. Nylandsted, *Cell Discovery*, 2021, **7**, 4.
28 G. M. Redpath, V. M. Betzler, P. Rossatti and J. Rossy, *Front. Cell Dev. Biol.*, 2020, **8**, 757.
29 N. Walani, J. Torres and A. Agrawal, *Proc. Natl. Acad. Sci. U. S. A.*, 2015, **112**, E1423–E1432.
30 A. J. Sodt, M. L. Sandar, K. Gawrisch, R. W. Pastor and E. Lyman, *J. Am. Chem. Soc.*, 2014, **136**, 725–732.